

# Attitude Estimation

Johnathan Clouse\*

*University of Colorado, Boulder, CO, 80309-0429, USA*

---

\*Graduate Student, Aerospace Engineering Sciences, 1111 Engineering Drive, Boulder, CO, 80309-0429

## Contents

|     |  |    |
|-----|--|----|
| I   | Introduction . . . . .                       | 3  |
| II  | Attitude Dynamics . . . . .                  | 3  |
| III | Simulation . . . . .                         | 4  |
| IV  | Filtering the Euler Representation . . . . . | 6  |
| V   | Multiplicative EKF . . . . .                 | 13 |
| VI  | Conclusion . . . . .                         | 15 |

## I. Introduction

Estimation of spacecraft attitude can provide solutions needed for control inputs. Many spacecraft have payloads that must be pointed in a specified direction to perform their function; attitude knowledge is the first step of that process.

Attitude can be represented in several ways. The most fundamental representation is a 3x3 direction cosine matrix, which can transform a vector from one frame to another. However, it has a total of nine elements. Euler angles can represent the same orientation in three elements. But, like all three-element representations, singularities can occur at certain rotations. Quaternions are representations that are universally non-singular, but they have four constrained elements.

This paper will identify the dynamics for a gravity gradient microsatellite. It will then detail two methods of attitude determination: an EKF estimating the Euler yaw-pitch-roll angles, and the Multiplicative EKF.

## II. Attitude Dynamics

The rotational equations of motion are given by Equation 1, where  $I_{xx}$  is the mass-moment of inertia about a principle axis and  $\omega$  is the body rate about that axis.

$$\begin{aligned} I_{11}\dot{\omega}_1 &= -(I_{33} - I_{22})\omega_2\omega_3 + T_1 \\ I_{22}\dot{\omega}_2 &= -(I_{11} - I_{33})\omega_3\omega_1 + T_2 \\ I_{33}\dot{\omega}_3 &= -(I_{22} - I_{11})\omega_1\omega_2 + T_3 \end{aligned} \quad (1)$$

The kinematic equation for a yaw-pitch-roll  $(\psi, \theta, \phi)$  representation is shown in Equation 2.<sup>1</sup> It is useful due to how the body rate vector  $\omega$  is separated, allowing for a change in Euler-angle representation if a singularity is being approached.

$$\begin{pmatrix} \dot{\psi} \\ \dot{\theta} \\ \dot{\phi} \end{pmatrix} = \frac{1}{\cos \theta} \begin{bmatrix} 0 & \sin \phi & \cos \phi \\ 0 & \cos \phi \cos \theta & -\sin \phi \cos \theta \\ \cos \theta & \sin \phi \sin \theta & \cos \phi \sin \theta \end{bmatrix} \begin{pmatrix} \omega_1 \\ \omega_2 \\ \omega_3 \end{pmatrix} = B(\psi, \theta, \phi)\omega \quad (2)$$

Gravity-gradient torque is given by Equation 3:<sup>1</sup>

$$\vec{T}_{grav} = \frac{3\mu}{R^5} \begin{pmatrix} R_2 R_3 (I_{33} - I_{22}) \\ R_1 R_3 (I_{11} - I_{33}) \\ R_1 R_2 (I_{22} - I_{11}) \end{pmatrix} \quad (3)$$

where  $\mu$  is Earth's gravitational parameter and  $R$  is the vector from the center of the Earth to the spacecraft center of mass, expressed in the body frame.  $R$  is obtained through inertial knowledge (either ephemeris or estimated) and rotated by the DCM in Equation 4.

$$DCM_{YPR} = \begin{bmatrix} \cos \theta \cos \psi & \cos \theta \sin \psi & -\sin \theta \\ \sin \phi \sin \theta \cos \psi - \cos \phi \sin \psi & \sin \phi \sin \theta \sin \psi + \cos \phi \cos \psi & \sin \phi \cos \theta \\ \cos \phi \sin \theta \cos \psi + \sin \phi \sin \psi & \cos \phi \sin \theta \sin \psi - \sin \phi \cos \psi & \cos \phi \cos \theta \end{bmatrix} \quad (4)$$

Combining the Equations 2, 3, and 4 lead to the kinematic Equation 5.<sup>1</sup>

$$\begin{pmatrix} \dot{\psi} \\ \dot{\theta} \\ \dot{\phi} \end{pmatrix} = B(\psi, \theta, \phi)\omega - \frac{\Omega}{\cos \theta} \begin{pmatrix} \sin \theta \sin \psi \\ -\cos \theta \cos \psi \\ -\sin \psi \end{pmatrix} \quad (5)$$

Equation 5 are the kinematics of a yaw-pitch-roll angle representation of attitude of the spacecraft body with respect to the Local Vertical, Local Horizontal (LVLH) frame. The LVLH frame in this paper is one where the vertical axis is anti-orbit-radial, and the cross-axis is anti-orbit-normal. This is the LVLH definition used by Johnson Space Center.

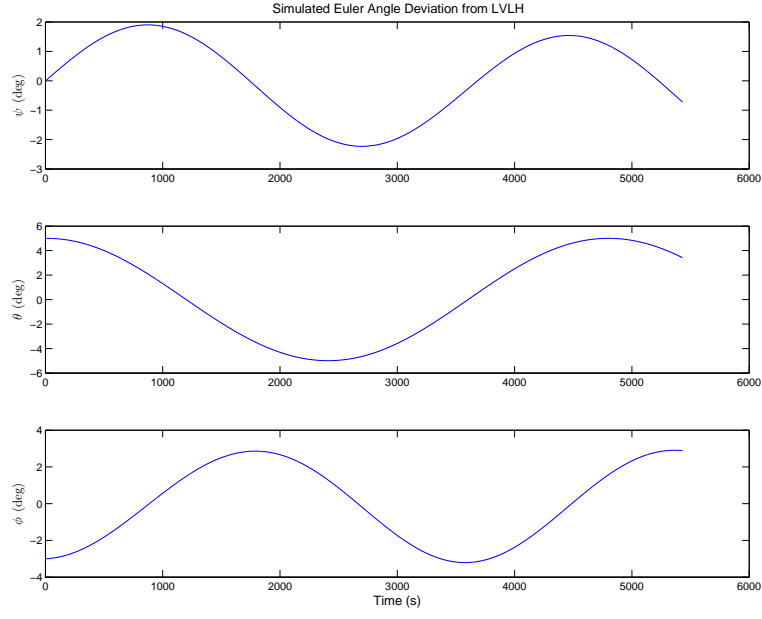
### III. Simulation

A microsatellite in low Earth orbit was simulated to provide data to be filtered. The simulated state was comprised of Earth-inertial position and velocity, the inertial-to-body quaternion, and the inertial rates expressed in the body frame. Position and velocity were propagated with a two-body point-mass model, while attitude was propagated with gravity gradient torque using Equations 1 and 3. Table 1 lists the parameter values that were used in the simulation.

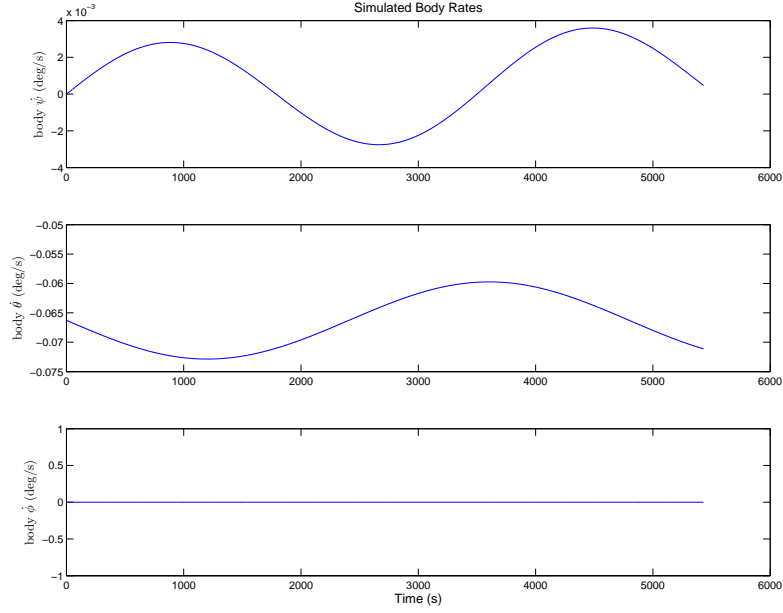
Table 1. Simulation Parameters

| Parameter                                   | Value      |
|---|------------|
| Orbit Semi-major axis                       | 6678 km    |
| Orbit Eccentricity                          | 0          |
| Orbit Inclination                           | 23°        |
| Orbit Arg of Periapse                       | 0°         |
| Orbit Right Ascension of the Ascending Node | 0°         |
| Initial true anomaly                        | 0°         |
| Spacecraft Mass                             | 50 kg      |
| Spacecraft Length                           | 0.5 m      |
| Spacecraft Width                            | 0.316 m    |
| $\mu_{Earth}$                               | 3.986e5 km |

The results of the simulation are shown in Figure 1 below.



(a) Euler angles wrt LVLH



(b) Body Rates

**Figure 1. Simulation results**

As expected, the gravity-gradient torque produced an oscillatory motion about the pitch and roll axes. The body yaw rate stays at zero due to the spacecraft symmetry, but the yaw in the euler representation is non-zero because it's a component of the attitude representation. This component changes with time due to the other components.

To simulate measurements, the rates were sampled at 1 Hz with noise of mean 0 rad/s and standard

deviation of 1e-6 rad/s. Direct Euler-angle measurements were also modeled, possibly from a composite attitude device (sun sensor with Earth sensor) or a (very coarse, as explained) star tracker. Noise was added with the model with mean  $0^\circ$  and standard deviation of  $0.165^\circ$ , applied about each Euler angle rotation.

#### IV. Filtering the Euler Representation

An Extended Kalman Filter was developed for estimating the Euler-angle representation of attitude from LVLH. The state being estimated was

$$X = \begin{pmatrix} \psi \\ \theta \\ \phi \\ \omega \end{pmatrix} \quad (6)$$

The dynamic model was linearized about  $X = 0$ , which is the equilibrium state for a gravity-gradient satellite. The direct attitude and rate measurements lead to simple measurement sensitivity matrices. For angles only:

$$H = \begin{bmatrix} I_{3 \times 3} & 0_{3 \times 3} \end{bmatrix} \quad (7)$$

For body rates only:

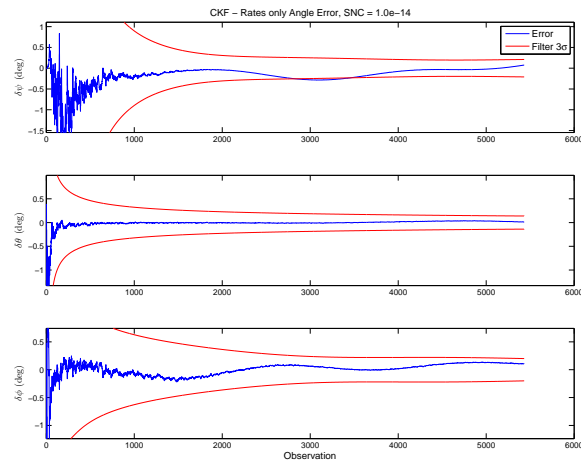
$$H = \begin{bmatrix} 0_{3 \times 3} & I_{3 \times 3} \end{bmatrix} \quad (8)$$

For both measurement types:

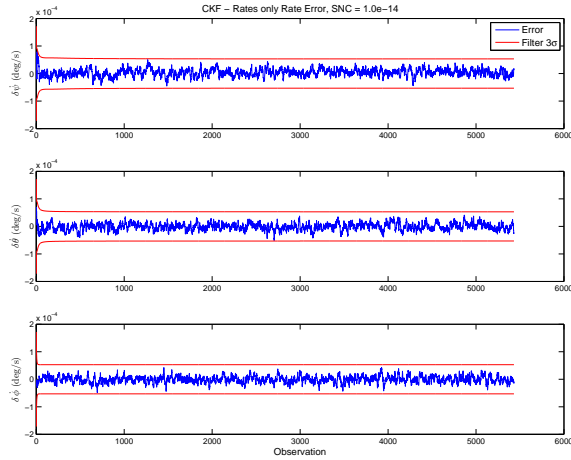
$$H = I_{6 \times 6} \quad (9)$$

All of these measurement sets make the system observable. The position and velocity states are not estimated; instead, they are propagated from ephemerides. These could be provided by ground-based observation and orbit determination.

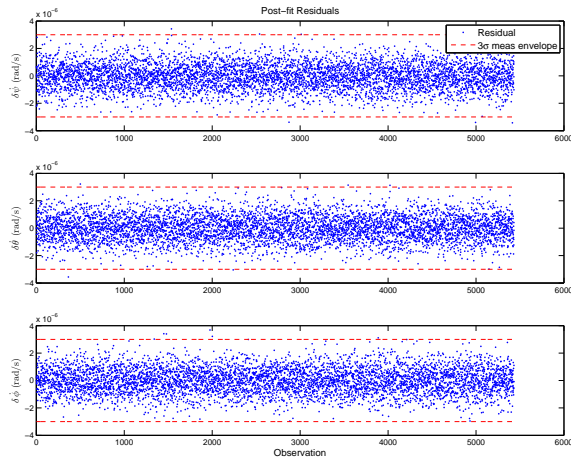
The first filter implementation of the Euler-angle filter, a conventional Kalman filter, was run with exact *a priori* state. Only rate measurements were used, and SNC variance of 1e-14 rad<sup>2</sup>/s<sup>2</sup> was implemented to abate the diminishing covariance. Figure 2 shows the results.



(a) Euler angle error



(b) Body rate error

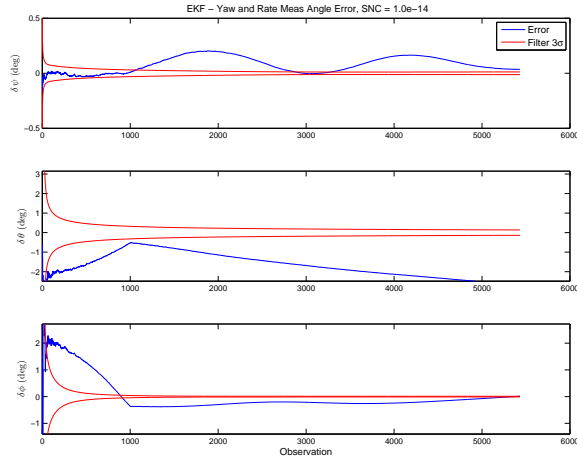


(c) Post-fit residuals.

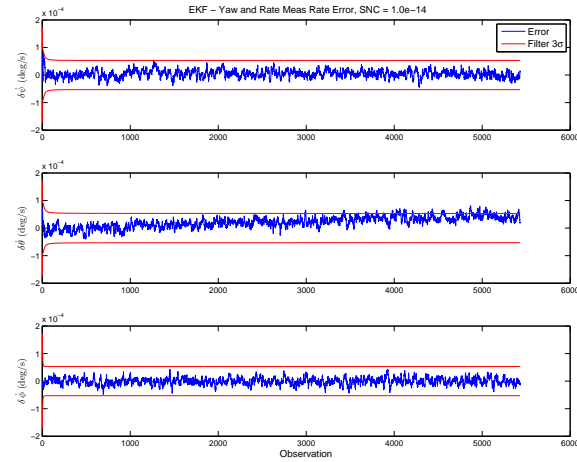
**Figure 2. Euler-angle CKF, exact *a priori* state, with rate measurements**

As one would expect, the resulting error was small and the filter fit to the measurement noise. However, the error did not remain completely within covariance envelope. The dynamic model cannot predict change in z-axis rate at all, because the symmetry of the spacecraft forces the angular acceleration to be zero in this axis.

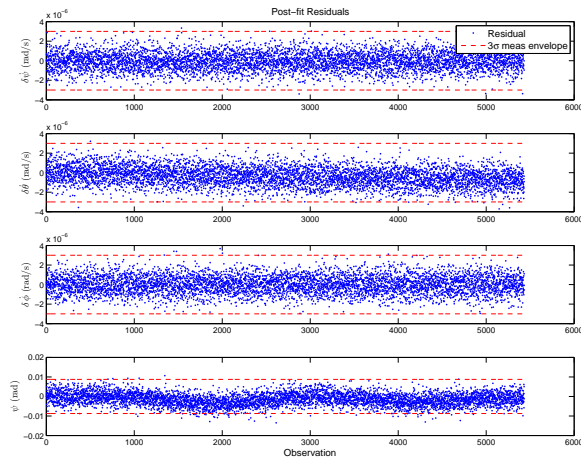
In order to gain more accuracy in the yaw solution, a yaw measurement was introduced. For this gravity-gradient spacecraft, such an observation could be realistically obtained by the spacecraft being in a sun-synchronous orbit. The extended Kalman filter was used after 1000 measurements, however, other values were considered and had the same result. Figure 3 shows the results.



(a) Euler angle error



(b) Body rate error

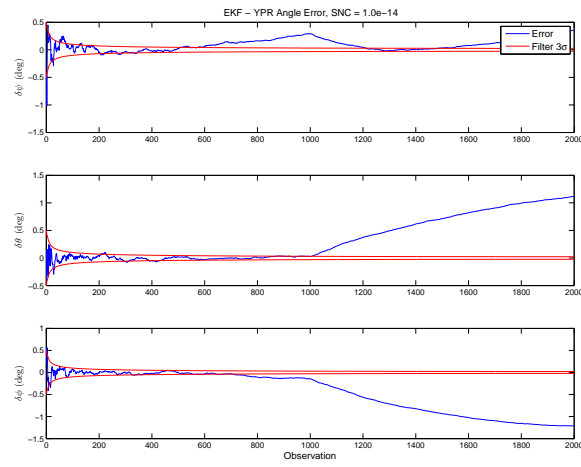


(c) Post-fit residuals.

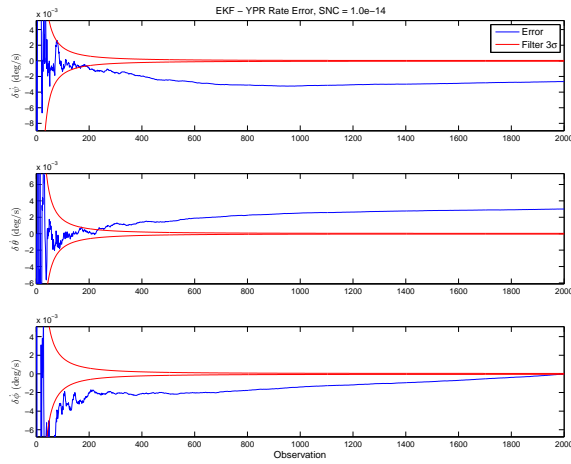
**Figure 3. Euler-angle EKF, exact *a priori* state, with yaw and body rate measurements**

The results are clearly poor. While yaw was initially more accurate, the pitch and roll errors stayed outside the covariance envelopes. The extended filter's state reset did not improve the estimate as desired. Further, the post-fit residuals do not match the noise.

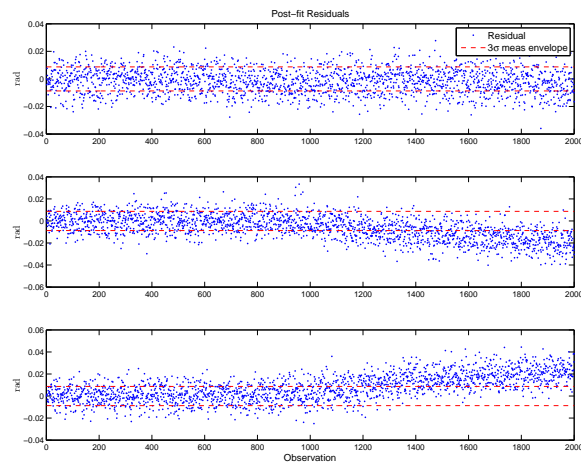
The direct attitude measurement was incorporated without the body rate measurements. SNC was tuned to be  $1\text{e-}16 \text{ rad}^2/\text{s}^2$  for the best post-fit residual result. Figure 4 shows the results.



(a) Euler angle error



(b) Body rate error



(c) Post-fit residuals.

Figure 4. Euler-angle EKF, exact *a priori* state, with yaw-pitch-roll measurements

The errors and residuals were, again, poor. The EKF did nothing to improve the state estimates. Pitch and roll diverged more after the EKF started.

Next, the direct attitude measurement and rate measurement were used by the filter. The exact *a priori* case was successful within the covariance envelope. The *a priori* state was set to  $X = 0$ , a good estimate as any for a nominally nadir-pointing spacecraft. The EKF was also started after 200 CKF-process observations. The results are shown in Figure 5.

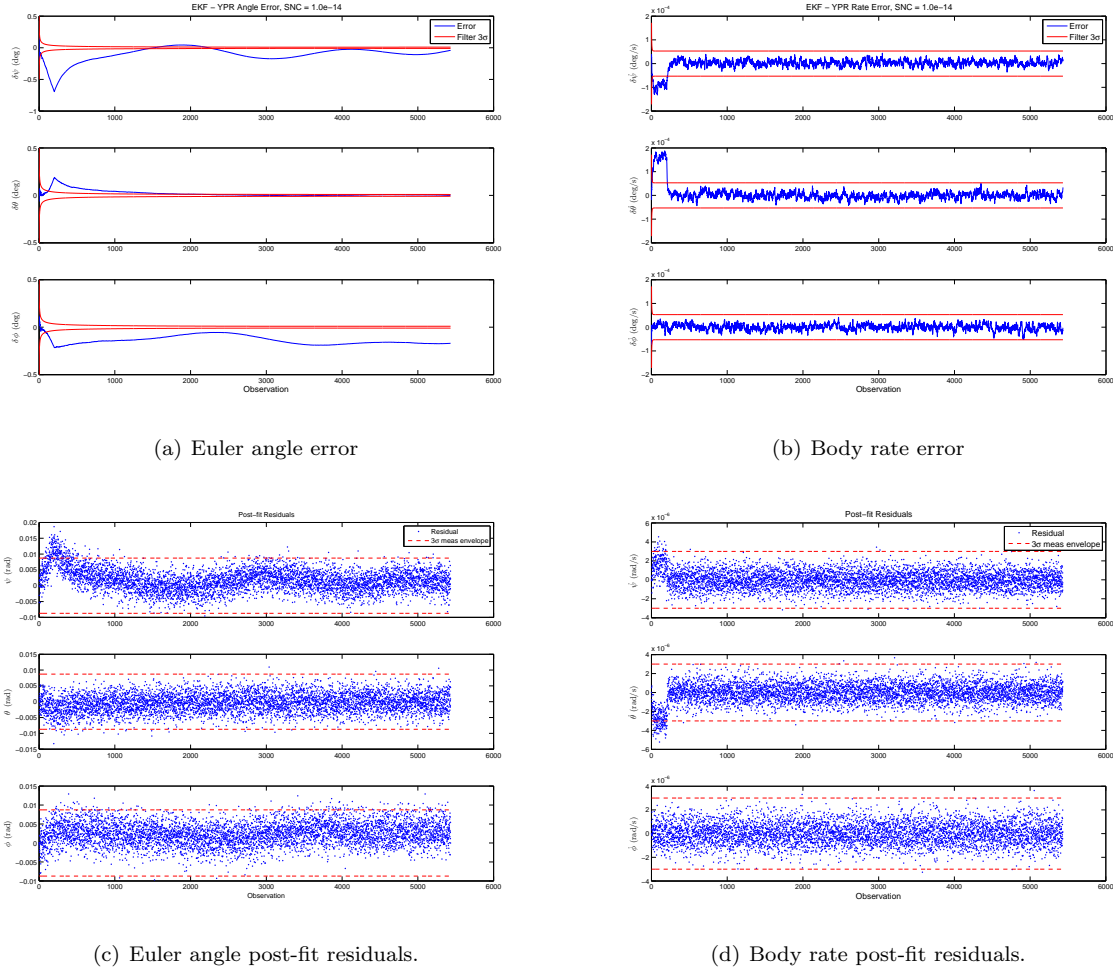


**Figure 5. Euler-angle EKF, *a priori* state  $X = 0$ , with yaw-pitch-roll and body rate measurements**

The filter results stay close to the truth value, however, they are outside of the covariance envelope much of the time. The post-fit residuals do not match the noise well.

As a final test of the capability of this Euler-angle filter, a 10-km error was introduced in the knowledge of the orbit altitude. Figure 6 shows how the error affected the filter estimate.

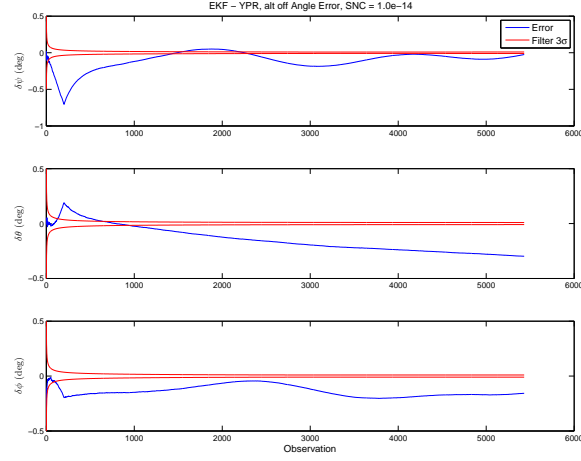


**Figure 6. Euler-angle EKF, exact *a priori* state, with yaw-pitch-roll measurements**

The estimated pitch diverges from the truth as time passes. The calculated orbit mean motion was affected by the increase in orbit altitude. The pitch was most affected by this error, as the LVLH frame with respect to the inertial frame changes by the mean motion, and the body is nominally aligned with pitch.

The Euler-angle filter proved difficult in getting good, meaningful results. While a singularity was avoided, the filter dynamics made it difficult to estimate the true attitude. A kinematic model that does not try to predict body rates may be of more use in this situation. This approach would make sense when the *a priori* state is the equilibrium state  $X = 0$ . When the spacecraft is in equilibrium, it is difficult to determine what the body rates are through the dynamic model. By using direct rate measurements, one could avoid this difficulty. However, rate gyro hardware does require knowing or estimating the bias about each axis.

## V. Multiplicative EKF

The Multiplicative EKF (MEKF) is useful in determining the attitude quaternion by estimating three parameters that represent a deviation from a propagated quaternion. Such parameters can include Rodriguez parameters, Euler vector and rotation, and the vector part of the quaternion. The latter representation was chosen for this effort. For the MEKF, the best estimate of the quaternion,  $\hat{q}$  given the estimate of the three-parameter representation  $\hat{\mathbf{a}}$  is<sup>2</sup>

$$\hat{q} = \delta q(\hat{\mathbf{a}}) \otimes q_{ref} \quad (10)$$

Equation 10 shows that the error quaternion  $\delta q$  represented by  $\hat{\mathbf{a}}$  is a rotation applied after the reference quaternion  $q_{ref}$  to get the best estimate of the true attitude quaternion. This equation is used in the state reset portion of the EKF. The error quaternion for the chosen representation of  $\hat{\mathbf{a}}$  is

$$\delta q(\mathbf{a}) = \frac{1}{2} \begin{bmatrix} \mathbf{a} \\ \sqrt{4 - a^2} \end{bmatrix} \quad (11)$$

Markley<sup>2</sup> shows that the covariance can be propagated as

$$\dot{P} = FP + PF^T + GQG^T - PHR^{-1}HP \quad (12)$$

where

$$F = \frac{\partial}{\partial a} \left( -\frac{1}{2} [\boldsymbol{\omega} \times] q_v \right) = -[\boldsymbol{\omega} \times] \quad (13)$$

is the linearization of the vector part quaternion propagation equation, resulting in the cross-product matrix for  $\boldsymbol{\omega}$ .  $G$  is simply identity for this case, and  $Q$  is the covariance matrix of the noise in the rates. The

product of these terms act as process noise, keeping the filter from saturating. Finally,  $H$  is the measurement sensitivity matrix, and  $R$  is the direct attitude measurement covariance.

Given a quaternion measurement, the measurement sensitivity matrix is  $H = I_{3 \times 3}$ . The measurement deviation  $y$  is computed by computing the successive rotations

$$\delta q(y) = q_{meas} \otimes q_{ref} \quad (14)$$

Equation 11 is applied to the result of 14 to put the measurement deviation into the specified parameter set. Care must be taken in this step, as  $q = -q$ . This means that the same attitude can be represented in two opposite quaternion representations, where the shortest rotation is the one with the positive scalar quaternion element. If the result of  $\delta q(y)$  is not close to the reference quaternion, the filter will display large divergence. However, the solution converges about the truth soon after. It is best to account for the discontinuity by using the smaller value of  $y$ .

The filter was implemented by feeding the body rate measurements directly into the kinematic model, rather than estimating them. The attitude measurement quaternion became the measurement the estimation was based on. Figure 7 shows the results.

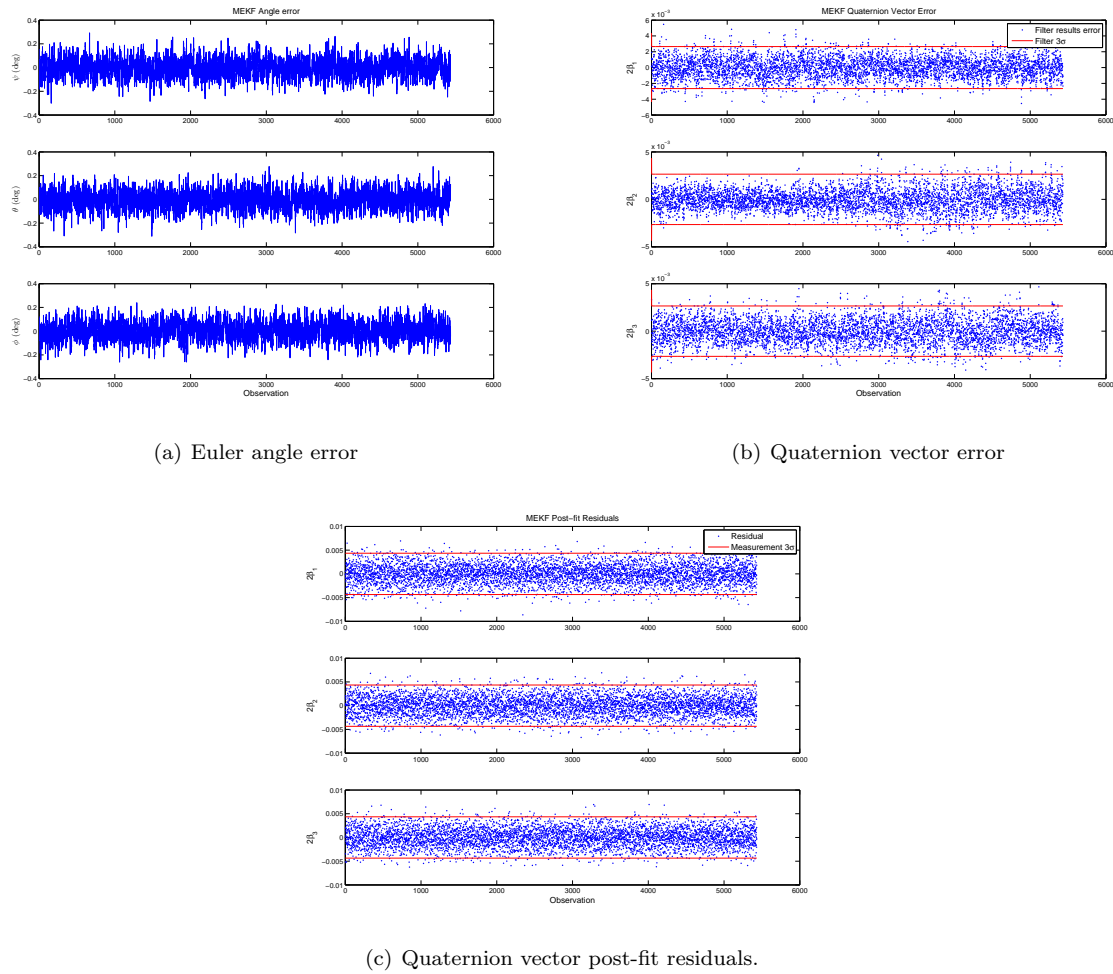


**Figure 7. Multiplicative EKF, *a priori* state  $X = 0$ , with attitude quaternion measurements**

The error of the estimation with respect to the true attitude was generally about zero. However, in the Euler-angle representation, one can see how noisy this error is compared to the Euler-angle EKF. The

post-fit residuals did not show any sign of bias or unaccounted systematic errors, but there were many points outside of the  $3\sigma$  measurement envelope.

Figure 8 shows results for measurements with  $\sigma = 0.033^\circ$ .

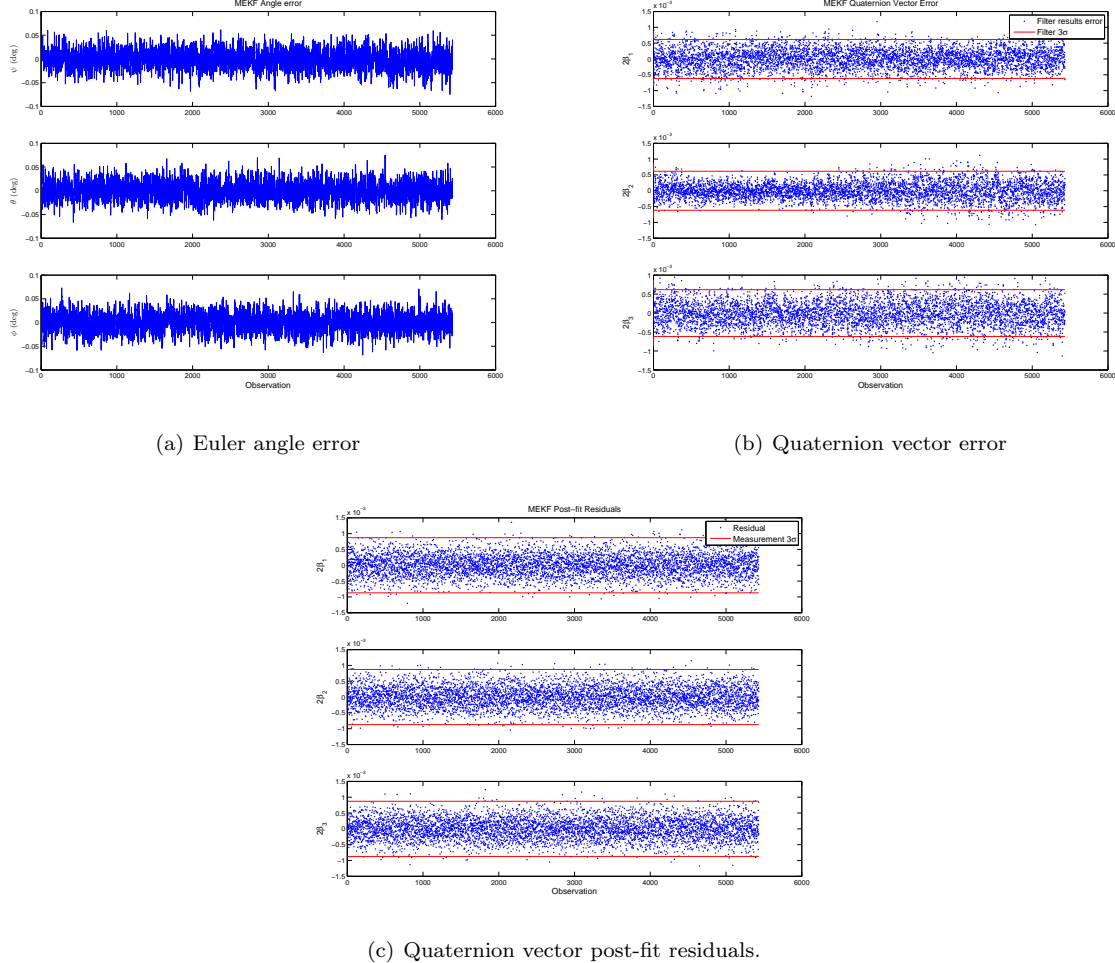


**Figure 8. Multiplicative EKF, *a priori* state  $X = 0$ , with attitude quaternion measurements.  $\sigma_{\text{meas}} = 0.033^\circ$**

Quantitatively, the filter behaved the same. Processing more precise measurements lead to more precision in the overall attitude error.

While this MEKF implementation was more accurate than the Euler-angle EKF, it was less precise given the same measurements. Such a solution would be more desirable for coarse control corrections, but not for high-precision tasks. This issue can be mitigated with a more precise sensor. This noisy error is thought to come from taking the body rates and feeding them into the filter kinematic model without estimating more accurate body rates.

## VI. Conclusion

Attitude estimation is quite different from orbit estimation. The usage of kinematics, rather than dynamics, generally makes it easier to estimate spacecraft attitude.<sup>3</sup> The constraints on attitude representation also make filter design more difficult.

Estimating the Euler angles was attempted due to the ease with which they can be understood. Kinematic equations exist for these representations, simplifying the direct calculation in the dynamic model that was used. Although the system was found to be observable with either direct attitude or rate measurements, in practice there was difficulty in converging on the true attitude. Using both measurement types constrained the filter to just follow the measurements. In addition, the noise may have been improperly applied to the yaw-pitch-roll attitude measurement, which may have introduced error into the filter that was not accounted for.

The MEKF, on the other hand, was very easy to implement following Markley's<sup>2</sup> method. This filter fit the data much better, and was able to give a more accurate estimation of the attitude. In reality, the gyro drift would also have to be estimated to keep the solution accurate. In addition, the error could probably be smoothed out if the body rates were sampled at a higher rate.

Attitude estimation was a tougher problem to tackle than I first thought. But it gave me several insights into estimation that do not exist in the orbit determination problem, namely state constraints and representation issues. In the end, I was able to use what I learned with the resources I found to estimate a gravity-gradient-stabilized spacecraft. It was an enjoyable project and I look forward to applying these techniques to other problems.

## References

<sup>1</sup>Schaub, H. and Junkins, J. L., *Analytical Mechanics of Space Systems*, AIAA, Reston, VA, 2nd ed., 2009.

<sup>2</sup>Markley, F. L., "Attitude Estimation or Quaternion Estimation?" *Flight Mechanics Symposium*, 2003.

<sup>3</sup>Markley, F. L., "Attitude Error Representations for Kalman Filtering," *Journal of Guidance, Control, and Dynamics*, Vol. 26, 2003, pp. 311–317.